From Pulsus to Pulseless: The Saga of Cardiac Alternans

James N. Weiss, Alain Karma, Yohannes Shiferaw, Peng-Sheng Chen, Alan Garfinkel and Zhilin Qu

Circ. Res. 2006;98;1244-1253
DOI: 10.1161/01.RES.0000224540.97431.f0
Circulation Research is published by the American Heart Association. 7272 Greenville Avenue, Dallas, TX 72514
 Print ISSN: 0009-7330. Online ISSN: 1524-4571

This Review is part of a thematic series on the **Biology of Cardiac Arrhythmias**, which includes the following articles:

Antiarrhythmic Drug Target Choices and Screening

Inherited Arrhythmogenic Diseases: The Complexity Beyond Monogenic Disorders

Genomics in Sudden Cardiac Death

Regulation of Ion Channel Expression

Biology of Cardiac Arrhythmias: Ion Channel Protein Trafficking

From Pulsus to Pulseless: The Saga of Cardiac Alternans

Eduardo Marbán and Gordon Tomaselli, Editors

***This series is in honor of Harry A. Fozzard, 8th Editor of* Circulation Research**

From Pulsus to Pulseless
The Saga of Cardiac Alternans

James N. Weiss, Alain Karma, Yohannes Shiferaw, Peng-Sheng Chen, Alan Garfinkel, Zhilin Qu

***Abstract*—**Computer simulations and nonlinear dynamics have provided invaluable tools for illuminating the underlying mechanisms of cardiac arrhythmias. Here, we review how this approach has led to major insights into the mechanisms of spatially discordant alternans, a key arrhythmogenic factor predisposing the heart to re-entry and lethal arrhythmias. During spatially discordant alternans, the action potential duration (APD) alternates out of phase in different regions of the heart, markedly enhancing dispersion of refractoriness so that ectopic beats have a high probability of inducing reentry. We show how, at the cellular level, instabilities in membrane voltage (ie, steep APD restitution slope) and intracellular Ca (Ca_i) cycling dynamics cause APD and the Ca_i transient to alternate and how the characteristics of alternans are affected by different "modes" of the bidirectional coupling between voltage and Ca_i. We illustrate how, at the tissue level, additional factors, such as conduction velocity restitution and ectopic beats, promote spatially discordant alternans. These insights have illuminated the mechanistic basis underlying the clinical association of cardiac alternans (eg, T wave alternans) with arrhythmia risk, which may lead to novel therapeutic approaches to avert sudden cardiac death. **(*Circ Res*. 2006;98:1244-1253.)**

Key Words: arrhythmias ■ alternans ■ heart failure ■ intracellular Ca cycling ■ electrical restitution

Sudden cardiac death (SCD) accounts for >300 000 deaths per year in the United States alone. Patients with reduced ejection fraction (<35%) are at greatest risk and are now routinely treated with implantable cardioverter defibrillators (ICDs).[1] Episodes of SCD attributable to the ventricular tachycardia (VT) and ventricular fibrillation (VF) remain highly unpredictable. Although ventricular ectopy is very common in these patients, the probability that a given premature ectopic beat(s) will induce lethal re-entry is extremely low. For example, 2 ectopic bpm, a common level of ventricular ectopy in such patients, equates to ≈1 million ectopic beats per year, yet SCD episodes in these patients occur over months to years, not minutes. The question that has puzzled cardiologists for decades is what makes that one-in-a-million ectopic beat so special? Scanning diastole with single or even

Original received February 17, 2006; revision received March 31, 2006; accepted April 19, 2006.

From the Departments of Medicine (Cardiology) (J.N.W., Y.S., A.G., Z.Q.) and Physiology (J.N.W.), David Geffen School of Medicine at UCLA, and Department of Physiological Science (A.G.), UCLA, Los Angeles, Calif; Division of Cardiology (P.-S.C.), Cedars-Sinai Medical Center, Los Angeles, Calif; Department of Physics and the Center for Interdisciplinary Research on Complex Systems (A.K.), Northeastern University, Boston, Mass.

Correspondence to James N. Weiss, MD, Division of Cardiology, 3645 MRL Building, David Geffen School of Medicine at UCLA, Los Angeles, CA 90095. E-mail jweiss@mednet.ucla.edu

***Circulation Research* is available at http://circres.ahajournals.org** **DOI: 10.1161/01.RES.0000224540.97431.f0**

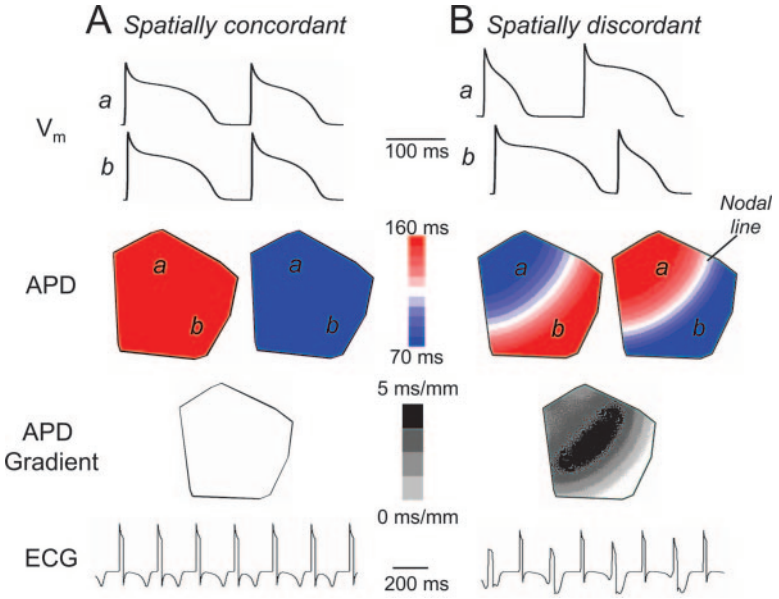

Figure 1. Spatially concordant (A) and discordant (B) APD alternans in simulated 2D cardiac tissue. A, Top traces show that simulated action potentials from sites *a* and *b* both alternate in a long-short pattern during pacing at 220-ms CL. Second panel shows that the spatial APD distribution is either long (blue) or short (red for each beat). Third panel shows that the APD dispersion (gray scale) for either long or short beats is minimal. Bottom panel shows simulated electrocardiogram (ECG), with T wave alternans. B, Top traces show that at a pacing CL of 180 ms, simulated action potentials from site *a* now alternate short-long, whereas at the same time, action potentials from site *b* alternate long–short. Second panel shows the spatial APD distribution, with a nodal line (white) with no APD alternation separating the out-of-phase top and bottom regions. Third panel shows that the APD dispersion is markedly enhanced, with the steepest gradient (black) located at the nodal line. Bottom panel shows simulated ECG, with both T wave and QRS alternans (attributable to engagement of CV restitution), as observed experimentally.[10] Simulations used a modified Luo–Rudy action potential model described previously.[11]

multiple premature ectopic beats during programmed electrical stimulation does not reliably induce VT/VF, particularly in the setting of nonischemic cardiomyopathy.[2] These findings suggest that a fixed arrhythmogenic substrate, just waiting for a properly timed trigger to occur to induce for VT/VF, is not the typical pathophysiological mechanism of SCD. Rather, they suggest that the tissue substrate changes dynamically so that only rarely does a trigger confront a substrate with the appropriate characteristics to initiate VT/VF.

Slow conduction and dispersion of refractoriness are the hallmarks of an arrhythmogenic substrate. Both are exacerbated in the diseased heart by structural and electrical remodeling and are modulated by autonomic tone, acute myocardial ischemia, electrolyte shifts, and drugs. Although a variety of dynamic factors influence this substrate, one that has received particular interest recently is cardiac alternans.

Electromechanical cardiac alternans refers to beat-to-beat alternation in the action potential duration (APD) and intracellular Ca (Ca_i) transient in a repeating pattern of long-short–long-short or large-small–large-small, respectively (Figure 1A). APD and the Ca_i transient typically alternate together (either in-phase or antiphase) because membrane voltage and Ca_i are bidirectionally coupled (ie, APD directly affects Ca_i transient amplitude, and, at the same time, the Ca_i transient amplitude directly affects APD via Ca-sensitive currents such as the L-type Ca current and electrogenic Na–Ca exchange).

Cardiac alternans in the form of pulsus alternans was first reported as a clinical sign of heart disease in a patient with alcoholic cardiomyopathy who died 2 months after his presentation[3] and was later described as an electrocardiographic T wave abnormality.[4] Subsequent experimental studies showed that mechanical and electrical alternans occur in many settings in which arrhythmias are also common, including acute myocardial ischemia, genetic channelopathies, and drug and electrolyte disturbances.[5] In the 1990s, human clinical trials conclusively established the link between cardiac alternans, in the form of electrocardiographic T wave alternans, and arrhythmia risk.[6,7] A recent multicenter clinical trial[8] has found that the absence of T wave alternans in patients with low ejection fractions may predict a low enough risk of SCD risk to obviate the need for an ICD.

In this review, we illustrate how the combination of mathematical modeling with experimental observations has represented a powerful approach for illuminating spatially discordant alternans as a potent arrhythmogenic mechanism. We show how spatially discordant cardiac alternans enhances the ability of ectopic beats to trigger re-entry and can also initiate VT/VF independently of ventricular ectopy in heterogeneous cardiac tissue. We discuss the dynamical mechanisms that cause APD and Ca_i alternans at the cellular level and show how these cellular mechanisms combine with additional factors to create spatially discordant alternans at the tissue level. Finally, we illustrate recent novel phenomena predicted from nonlinear interactions between action potential and Ca_i cycling dynamics, which may be relevant both to the initiation and maintenance of VT/VF observed experimentally.

Cardiac Alternans and SCD

Cardiac alternans may be spatially concordant or discordant. In the spatially concordant case (Figure 1A), all regions of the tissue alternate in phase with each other (ie, for a given beat, the APD [or Ca_i transient] is either long [large] or short [small] everywhere in the tissue). However, in the spatially discordant case (Figure 1B), some regions of tissue alternate in a long-short-long pattern, whereas other regions simultaneously alternate in a short-long-short pattern. These out-of-phase regions are separated by a nodal line, in which no alternans is present. At a nodal line, the spatial gradients in APD or Ca_i transient amplitude are the steepest, predisposing to localized conduction block.[9–12]

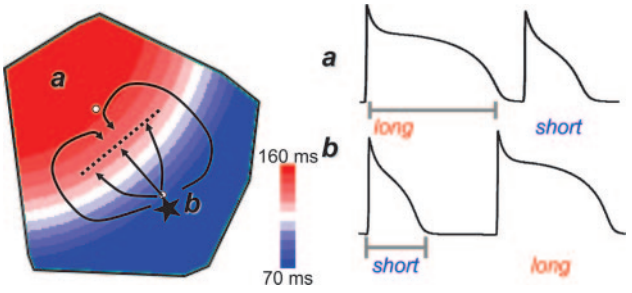

Figure 2. Mechanism of initiation of re-entry by a premature ectopic beat during spatially discordant alternans. A premature ectopic beat (asterisk) occurring in the region of short APD blocks (black line) as it propagates across the nodal line into the region with long APD. Meanwhile, the ectopic beat successfully propagates laterally, waiting for the long APD region to repolarize and then re-enters the blocked region to initiate figure-eight re-entry.

Spatially concordant APD alternans is less arrhythmogenic than spatially discordant APD alternans.[10,11] Although APD and hence refractory period alternate, for any given beat, the refractory period is either long or short everywhere, and hence dispersion of refractoriness is not greatly amplified. However, once APD alternans becomes spatially discordant, dispersion of refractoriness is greatly amplified, producing a favorable substrate for initiation of re-entry by an ectopic beat, as illustrated in Figure 2. Moreover, if the tissue is heterogeneous such that some regions are inherently more susceptible to alternans than other regions,[13] then re-entry can occur even in the absence of a premature ectopic beat.[10,11,14] This is because amplitude of alternans can grow only so large before the diastolic interval (DI) after the long APD shrinks to zero, resulting in conduction block of the next wavefront (with short APD). When 2:1 conduction failure occurs locally in the region with high susceptibility to alternans, unblocked impulses from adjacent low susceptibility regions can re-enter to blocked region, inducing figure-eight re-entry (by the same scenario in Figure 2 but without the premature ectopic beat). This is the typical mechanism by which rapid ventricular pacing induces VF, as has been documented in both experimental optical mapping studies[10,14] and simulations.[11]

In conclusion, when spatially discordant alternans occurs, dispersion of refractoriness is dynamically enhanced to a marked extent, making the tissue highly vulnerable to initiation of reentry.

The Cellular Basis of Cardiac Alternans

APD Restitution Slope

In their landmark 1968 article on cardiac alternans, Nolasco and Dahlen[15] intuitively explained the relationship between APD alternans and APD restitution slope. APD restitution refers to the relationship between APD and the previous DI, which can be measured experimentally by plotting APD versus DI as the heart rate increases. Drawing an analogy to electronic feedback circuits, Nolasco and Dahlen used a simple graphical method to demonstrate that

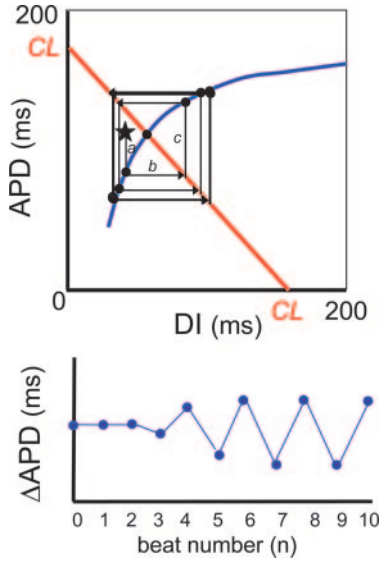

Figure 3. Cobweb diagram of APD alternans arising from steep APD restitution slope, after Nolasco and Dahlen.[15] Blue line shows the APD restitution curve, and red line shows the CL=APD+DI line. The top graph illustrates the effects of a perturbation, which shortens DI (asterisk), displacing the system from its unstable equilibrium point (solid black circle at the intersection of the two lines), resulting in persistent APD alternans, as shown in the bottom trace. See text for details.

sustained APD alternans occurs when APD restitution slope is >1 at a given cycle length (CL). Figure 3 (top) shows a typical APD restitution curve, for which $APD_{n+1}=f(DI_n)$, where f is the function relating the new APD (APD_{n+1}) to the previous DI (DI_n). For pacing at a constant CL, the relationship $CL=APD_n+DI_n$ can be illustrated on the same graph as a straight line with slope of −1. The intersection of the two lines is an equilibrium point satisfying both equations. Whether APD alternates at this CL depends on whether this equilibrium point is stable or unstable. The local stability can be determined by perturbing the DI by a small amount δ, such that $DI_{n+1}=DI_n+\delta$. Graphically, for a negative value of δ (which shortens DI), this moves DI_{n+1} to the left on Figure 3 (top, indicated by the star). The shorter DI_{n+1} will cause a shorter APD_{n+2}, the value of which can be determined by dropping a vertical line (labeled *a*) to the intersection with the APD restitution curve. However, the shorter APD_{n+2} will create a long DI_{n+2}, the value of which can be determined by drawing a horizontal line (labeled *b*) to its intersection with the CL line. This value of DI_{n+2} will, in turn, produce a long APD_{n+3}, the value of which is determined by the intersection of the vertical line *c* with the APD restitution curve and so forth. In this example, the amplitude of APD alternans progressively increases, finally equilibrating at a steady-state alternans, indicating that the equilibrium point is unstable. It can be readily shown[15] that if the slope of the APD restitution curve at its intersection with the CL line is <1, APD alternans will be transient and return to the stable equilibrium point over successive beats. However, if the slope is >1, the equilibrium point is unstable, and the amplitude of APD alternans

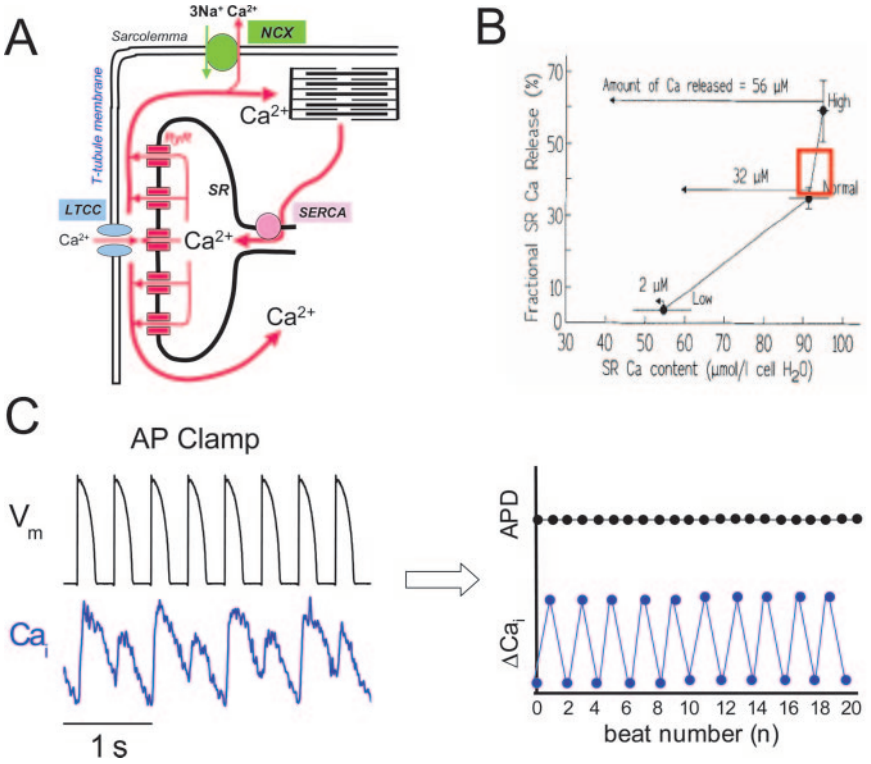

Figure 4. Ca_i cycling dynamics in cardiac myocytes. A, Schematic of Ca_i cycling, illustrating that a small amount of Ca entering the cell through L-type Ca channels (LTCC) triggers release of a large amount of Ca from internal stores (SR) by activating SR Ca release channels (ryanodine receptors [RyR]). Ca is then pumped back into the SR by SERCA pumps, or removed from the cell by Na–Ca exchange (NCX). B, Experimental measurement of fractional SR Ca release as a function of the SR Ca load, reproduced with permission from Bassani et al.[29] The release slope (*m*) increases with SR Ca load. C, Demonstration of primary Ca_i alternans in an isolated rabbit ventricular myocyte. Despite clamping membrane voltage with a constant action potential (AP) waveform to prevent beat-to-beat APD alternans, the Ca_i transient still alternated. Modified with permission from Chudin et al.[21]

will grow. This can either lead to 2:1 block or to stable APD alternans, as in the case shown, if a flat region of APD restitution exists at long DI to limit progressive expansion of alternans amplitude. For nonmonotonic APD restitution curves, which have been recorded in humans and other species in some studies,[16] more complex dynamics, including chaotic beat-to-beat APD variation during 1:1 capture, may occur,[17] although the physiological relevance is unclear.

Although conceptually very useful and well supported by computer simulations, this analysis of APD alternans has several limitations when applied to real cardiac tissue because the cellular and molecular mechanisms of APD restitution and APD alternans are multifactorial. The assumption that APD is solely a function of the previous DI is an oversimplification because the pacing history is also important (termed short-term cardiac memory, or APD accommodation). Memory effects have been shown to limit the reliability of the APD restitution slope >1 criterion in predicting the onset of APD alternans.[18] Most important, Ca_i cycling dynamics has been recognized recently to play a key role in the genesis of APD alternans,[19,20] as described in the next section.

Ca_i Cycling Dynamics

Membrane voltage and Ca_i are bidirectionally coupled in cardiac tissue. With respect to the influence of voltage on Ca_i (V→Ca coupling), the L-type Ca current is a major determinant of both APD and Ca_i transient amplitude, so that if APD alternates because of steep APD restitution, the Ca_i transient amplitude will also alternate secondarily in response to the alternating L-type Ca current amplitude. Conversely, for Ca→V coupling, the Ca_i transient amplitude strongly modulates APD through its effects on Ca-sensitive currents during the action potential plateau (Figure 4A). Whereas V→Ca coupling is generally positive (ie, a longer APD produces a larger Ca_i transient), Ca→V coupling can be either positive or negative. Positive Ca→V coupling refers to the mode in which a larger Ca_i transient produces a longer APD. This occurs when the large Ca_i transient enhances net inward current during the action potential plateau by potentiating inward Na–Ca exchange current to a greater extent than it reduces the L-type Ca current (by facilitating Ca-induced inactivation). On the other hand, negative Ca→V coupling refers to the mode in which a larger Ca_i transient causes a shorter APD. This occurs when the reduction in L-type Ca current predominates over the increased Na–Ca exchange current. Other Ca-sensitive currents, such as the Ca-activated nonselective cation current and Ca-activated Cl currents, also modulate the strength of Ca→V coupling by affecting APD but are quantitatively less important. Therefore, if a dynamic instability causes the Ca_i transient to alternate, then the APD will passively follow suit and also begin to alternate and vice versa.

Because recent voltage clamp experiments[21–24] have documented that Ca_i transients in isolated myocytes can exhibit profound alternans despite a constant voltage waveform (Figure 4C), the question arises as to whether APD alternans is typically driven by voltage dynamics (ie, steep APD restitution slope) or Ca_i-cycling dynamics under physiological conditions. Mounting experimental evidence indicates that the onset of APD alternans is primarily attributable to an instability in Ca_i cycling dynamics rather than steep APD restitution. In both intact tissue[25] and isolated ventricular myocytes,[20] the onset of APD alternans occurred at a pacing CL at which APD

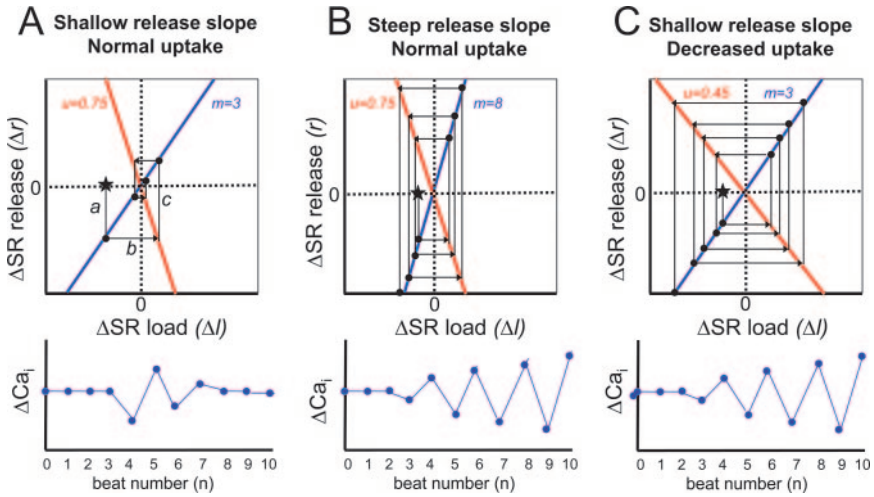

Figure 5. Cobweb diagram of Ca_i alternans. A, Blue line shows the relationship between SR Ca release vs SR Ca load, with slope m in Equation 1. Red line indicates the conservation of Ca between beats as a function of SR Ca release slope (m) and sequestration efficiency (u) in Equation 2. The top graph illustrates the effects of a perturbation that induces a change in SR Ca load (asterisk), displacing the system from its equilibrium point (solid black circle at the intersection of the two lines). For $m=3$ and $u=0.75$ (normal heart), the beat-to-beat change in SR Ca release converges back to its equilibrium value over the ensuing beats. See text for details. B, In contrast, when $m=8$ (corresponding an increase in fractional SR Ca release slope), the equilibrium point becomes unstable, and alternans grows with each beat, although u is unchanged. C, Unstable alternans also occurs when m remains low[3] but u decreases (0.45), indicating reduced SR Ca sequestration efficiency.

restitution slope was still considerably <1 and interventions that suppressed sarcoplasmic reticulum (SR) Ca_i cycling invariably eliminated APD alternans, sometimes irrespective of their effect of APD restitution.[20] Moreover, Pruvot et al[19] found that in intact ventricle, the endocardium, despite having a flatter APD restitution slope than the epicardium, developed APD alternans first, which they subsequently ascribed to differences in Ca_i cycling properties between endocardial and epicardial myocytes.[13] Finally, acute ischemia causes APD and mechanical alternans at normal heart rates,[26,27] yet it flattens APD restitution slope.[26]

Recent studies have investigated the factors causing dynamical instability in Ca_i cycling leading to Ca_i transient alternans. Diaz et al[24] proposed that the primary cause is a steep dependence of SR Ca release on SR Ca load. In a more extensive theoretical treatment by Shiferaw et al,[28] SR Ca uptake has been identified as a key additional factor. To provide an intuitive understanding of factors promoting Ca_i transient alternans, we adapted the graphical approach used by Nolasco and Dahlen[15] to Ca_i cycling (Figure 5), after the reduction of the Ca_i cycling dynamics to iterative maps by Shiferaw et al.[28] During the cardiac action potential, a small influx of Ca through L-type Ca channels triggers release of a much larger amount of Ca stored in the SR via the process of Ca-induced Ca release illustrated in Figure 4A. Moreover, the fractional release of SR Ca increases with SR Ca load,[29] as shown by the experimental curve in Figure 4B. If we consider a given region of this curve (eg, the red square), then for the nth beat, the change in SR Ca release ($\Delta r_n = r_n - r_{n-1}$) can be represented as a function of the change in SR Ca load ($\Delta l_n = l_n - l_{n-1}$) by the equation

$$\Delta r_n = m\Delta l_n, \quad (1)$$

where m is the slope of the relationship between SR release and SR load (assumed here to be linear and positive). After Ca release on the n^{th} beat, the amount of Ca left in the SR is $l_n - r_n$, and the amount in the cytoplasm is then $t - l_n + r_n$, where t is the total Ca in the myocyte. For the next $(n+1)$ beat, the SR Ca load will then equal the amount left in the SR from the previous beat, plus the net amount taken back up into the SR, $u(t - l_n + r_n)$, where u is defined as the SR Ca requestration factor and can range from 0 to 1. Accordingly,

$$l_{n+1} = l_n - r_n + u(t - l_n + r_n) \quad (2)$$

$$l_n = l_{n-1} - r_{n-1} + u(t - l_{n-1} + r_{n-1})$$

$$\Delta l_{n+1} = \Delta l_n - \Delta r_n + u(-l_n + \Delta r_n)$$

$$\Delta l_{n+1} = (1-u)(\Delta l_n - \Delta r_n)$$

Substituting Equation 1:

$$\Delta l_{n+1} = -(m-1)(1-u)/m \times \Delta r_n \quad (3)$$

leading to

$$\Delta r_n = -m/(m-1)(1-u) \times \Delta l_{n+1}. \quad (4)$$

Both Equation 1 and Equation 4 are straight lines that pass through the origin, with slopes of m and $-m/(m-1)(1-u)$, respectively. Their intersection (at [0, 0]) represents an equilibrium point (Figure 5). As in the case of APD restitution (Figure 3), the stability of the equilibrium can be determined by perturbing the change in SR Ca load by a small amount δ, such that $\Delta l_{n+1} = \Delta l_n + \delta$. As shown graphically in Figure 5A, a small negative δ moves Δl_{n+1} to the left (indicated by the star). The smaller change in SR load Δl_{n+1} will cause a smaller change in SR release Δr_{n+1}, the value of which can be determined by dropping a vertical line (labeled a) to the intersection with the Equation 1 release curve. However, the smaller change in SR release Δr_{n+1} will result in a larger change in SR load Δl_{n+2}, the value of which can be determined by drawing a horizontal line (labeled b) to its intersection with the Equation 2 line. This larger value of Δl_{n+2} in turn produces a larger Δr_{n+2}, the value of which is determined by the intersection of the vertical line c with the Equation 1 release curve, and so forth. In Figure 5A, with shallow SR Ca release slope ($m=3$) and robust SR Ca sequestration ($u=0.75$), the equilibrium is stable so that the

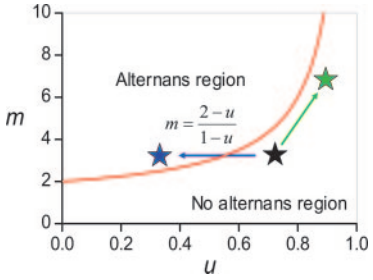

Figure 6. Ca_i cycling stability. Stability analysis predicts that the curve $m=(2-u)/(1-u)$ represents the boundary between stability (no alternans) and instability (alternans). The basal state of the normal heart is indicated by the black star. β-Adrenergic stimulation (green star) increases both m (fractional SR Ca release) and u (SR Ca sequestration), the latter protecting the heart from Ca_i alternans. Heart failure or acute ischemia (blue star) primarily decrease u, pushing the heart into the alternans regime even at normal heart rates, hypothetically accounting for pulsus alternans, T wave alternans, and increased arrhythmia risk.

Ca_i alternans is only transient and returns to the equilibrium point with successive iterations. However, in Figure 5B, in which the SR Ca release slope has been increased ($m=8$) with the same SR Ca sequestration factor ($u=0.75$), the equilibrium is unstable so that Ca_i alternans amplitude expands progressively with each beat. Alternans can either increase to the point at which release occurs only on every other beat (2:1 release block) or can reach a state of stable alternans when the small SR Ca releases extend into the flat (small m) region of the release curve in Figure 4B, analogous to Figure 3. To illustrate the importance of SR Ca sequestration, Figure 5C shows the case in which SR Ca release slope remains shallow ($m=3$) but SR Ca sequestration is decreased ($u=0.45$). This again produces an unstable equilibrium so that Ca_i alternans expands progressively.

Thus, unlike voltage-driven alternans in Figure 3, in which a single parameter (APD restitution slope) controls alternans instability, for Ca_i-driven alternans, two parameters play equally important roles: m, the slope of the SR Ca release versus SR Ca load, and u, the efficiency of SR Ca sequestration.[28] Although u is a phenomenological parameter, physiologically, its value intuitively depends on two factors: the rate of Ca uptake into the SR by the sarcoplasmic–endoplasmic reticulum Ca ATPase (SERCA) pump, and Ca leak from the SR via ryanodine receptors or other leak pathways. Figure 6 summarizes how the relative values of m and u jointly control the threshold for Ca_i alternans. This relationship is derived by substituting Equation 1 into Equation 2 as follows:

$$\Delta l_{n+1}=(1-u)(\Delta l_n-m\Delta l_n)$$

$$\Delta l_{n+1}=-\Delta l_n(m-1)(1-u),$$

which, by iteration, gives:

$$\Delta l_n=\Delta l_0[-(m-1)(1-u)]^n. \quad (5)$$

Equation 5 predicts that the onset of alternans occurs when the quantity in brackets raised to n^{th} power is less than minus unity (ie, $-(m-1)(1-u)<-1$, or $(m-1)(1-u)>1$, which is the condition for the magnitude of the SR load perturbation Δl_n to grow exponentially with increasing beat number and for the sign of Δl_n to alternate from beat to beat.

The physiological implications of Figure 6 for conditions such as acute β-adrenergic stimulation, heart failure, and acute ischemia are intriguing. During acute β-adrenergic stimulation, enhancement of SR Ca uptake by the SERCA pump increases both the SR Ca load and the fractional SR release (ie, m increases), which tends to promote alternans. However, SERCA pump stimulation also increases u even more steeply, protecting against Ca_i alternans (Figure 6, green star), consistent with experimental observations that a higher heart rate is required to induce APD alternans after isoproterenol.[30,31] On the other hand, during chronic heart failure, reduced SERCA expression and increased SR Ca leak through hyperphosphorylated ryanodine receptors (SR Ca release channels)[32] may decrease u sufficiently to promote Ca_i alternans at near-normal heart rates, although m remains near normal (blue star). This may account for the observation of pulsus alternans in advanced heart failure as well as T wave alternans and increased arrhythmia risk. During acute ischemia, SR Ca load remains normal, but SERCA pump activity decreases markedly, which also decreases u to promote alternans at normal heart rates (blue star).[26,27]

However, a caveat in extrapolating these theoretical predictions to the physiological setting is that the linear stability analysis is valid only in the immediate vicinity of the equilibrium point; that is, once Ca_i alternans becomes appreciable, the total Ca t in the myocyte fluctuates on a beat-to-beat basis, violating the assumption that t is constant.

Interactions Between Voltage- and Ca_i-Driven Instabilities

Because the coupling between APD and the Ca_i transient is bidirectional, an important question is how the voltage-driven and Ca_i-driven instabilities interact with each other to affect the onset and pattern of cellular alternans. This issue has recently been studied theoretically by Shiferaw et al.[33] When V→Ca and Ca→V coupling are both positive (ie, a longer APD promotes a larger Ca_i transient at the same time that a larger Ca_i transient promotes a longer APD), the interaction is synergistic, so that the onset of the alternans instability occurs sooner. For example, the onset of APD and Ca_i alternans may occur when APD restitution slope is still <1.

The more interesting case occurs when V→Ca is positive and Ca→V coupling is negative (ie, a long APD promotes a large Ca_i transient, but a large Ca_i transient promotes APD shortening). In this case, the two dynamical instabilities oppose each other, each inhibiting the other's ability to cause alternans. When alternans does occur, its pattern depends on which instability predominates. If alternans is primarily voltage driven by steep APD restitution slope, APD and Ca_i transient alternans are electromechanically concordant (long APD associated with large Ca_i transient), but when Ca_i driven, it is electromechanically discordant (long APD associated with small Ca_i transient). When the voltage and Ca_i instabilities are more equally balanced, the pattern of alternans becomes quasiperiodic (ie, APD and Ca_i transient alternans fluctuate in both their amplitudes and degree of electromechanical concordance/discordance). Quasiperiodic

patterns consistent with this mechanism has been reported in Purkinje fibers.[34,35]

Although only positive V→Ca coupling has been studied in simulations to date, it is also conceivable that negative V→Ca may occur, for example, in myocytes expressing a high level of the transient outward current I_{to} (eg, atrial or ventricular epicardial cells). In this case, the large I_{to} could enhance the Ca_i transient by increasing the driving force for Ca entry through L-type Ca channels,[36,37] while shortening APD. The dynamic consequences of this case have yet to be investigated.

Alternans in Cardiac Tissue

At the tissue level, both voltage- and Ca_i-driven alternans can lead to formation of spatially discordant alternans. Originally, spatially discordant APD alternans was thought to be created by pre-existing APD gradients because cardiac tissue is inherently heterogeneous.[10] However, computer simulations subsequently suggested that tissue heterogeneity is not required for the formation of spatially discordant alternans.[9,11] In homogeneous tissue paced at increasing rates, two classic mechanisms that can create spatially discordant alternans are engagement of conduction of velocity (CV) restitution and a premature ectopic beat arising from a different location.

Spatially Discordant Alternans Attributable to CV Restitution

CV, like APD, is also sensitive to the preceding DI, which is called CV restitution, analogous to APD restitution. CV restitution is typically flat at long DI but decreases at short DI because of incomplete recovery from inactivation of Na channels. Figure 7A illustrates how rapid pacing sufficient to engage the sloped region of CV restitution curve converts spatially concordant alternans into spatially discordant alternans. In this example, spatially concordant alternans was first induced by rapid pacing from the top of the cable. When the pacing rate was further increased (beats A0–A1), the DI after beat A0 (with long APD) became short enough to engage CV restitution, slowing the CV of beat A1 as it propagated down the cable. The slowing of conduction allowed the DI to lengthen slightly toward the bottom of the cable, which caused APD toward the bottom to lengthen slightly. This process self-amplified during subsequent beats, eventually evolving into the steady-state pattern of spatially discordant APD alternans shown in the beats to the right. Thus, the CL at which CV restitution is engaged becomes a major determinant of the conversion of spatially concordant alternans to spatially discordant alternans. During acute and chronic ischemia, Na channel recovery from inactivation becomes delayed,[38–40] enhancing the range of DI over which CV varies, which may be a major factor promoting spatially discordant alternans and increased arrhythmia risk in these settings.[41] During acute ischemia, spatially discordant alternans can even occur at normal heart rates.[27]

Spatially Discordant Alternans Attributable to an Ectopic Beat

Figure 7B illustrates the second mechanism in a simulated 1D cable of homogeneous cardiac cells. When the cable was paced from the top (first beat), a premature stimulus delivered at the bottom of the cable after a short DI (second beat) created an asymmetric distribution of DI for the next paced beat arising from the top of the cable (third beat). In response to this gradient in DI, the APD of the next paced beat (fourth beat) was short at the top but long at the bottom, causing the next APD to be short at the top and long at the bottom and so forth.

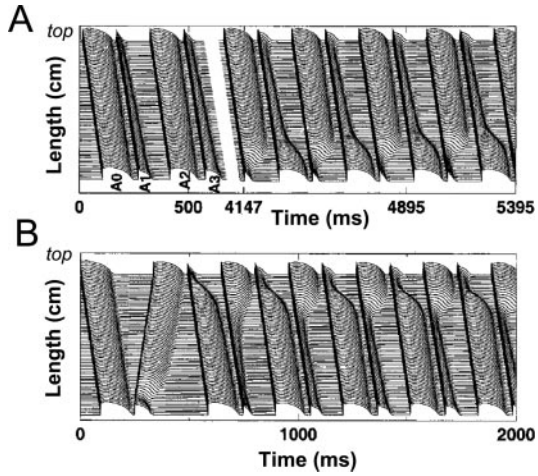

Figure 7. Formation of spatially discordant alternans by CV restitution (A) or an ectopic beat (B). Superimposed traces of membrane voltage vs time show action potential (AP) characteristics along the length of a simulated 1D cable of cardiac cells, stimulated at the top of the cable and propagating to the bottom with a wavefront velocity (CV) corresponding to the slope of the line formed by the AP upstrokes. A, CV restitution mechanism: spatially concordant APD alternans is already present when the pacing rate is increased further to engage CV restitution. The slowed CV causes the DI to increase slightly but progressively as the impulse propagates from the top to the bottom of the cable, creating dispersion of APD that is amplified during the subsequent beats until reaching a maintained steady state. Note that the pattern, once formed, is maintained indefinitely (right panels). See text for details. B, Ectopic beat mechanism: an ectopic beat arising from a different location (the bottom of the cable) creates the gradient in DI from top to bottom, which induces spatially nonuniform APD alternans. See text for details. The spatially discordance is transient, unlike the CV restitution mechanism. Adapted with permission from Watanabe et al.[9]

Simulations show that in heterogeneous tissue with a pre-existing APD gradient, spatially discordant alternans does not occur during rapid pacing at a constant CL in the absence of CV restitution. However, spatially discordant APD alternans can arise if the pacing CL is suddenly changed. In this case, there is no requirement to pace at different sites because the pre-existing APD heterogeneity is sufficient to break the symmetry of DIs, unlike that homogenous tissue case, in which pacing from a different site is required.

In both of these cases, the pattern of spatially discordant alternans is transient and eventually returns to spatial concordance, unlike the CV restitution mechanism.

Role of Electrotonic Coupling on the Nodal Line Spacing

Ionic model simulations have revealed that CV restitution causes several equally spaced nodal lines to form in spatially

extended homogeneous tissue.[9] The spacing between nodal lines is crucially important because it determines the minimum size of cardiac tissue necessary to form discordant alternans by CV restitution, which turns out to be roughly one quarter of the natural spacing between nodes.[28] Furthermore, a smaller spacing between nodes produces a steeper spatial gradient of refractoriness during discordant alternans of the same amplitude and hence makes the substrate more arrhythmogenic. Mathematical analysis by Echebarria and Karma[42] has demonstrated that the spacing between nodal lines is determined both by the steepness of the CV–restitution curve and the strength of electrotonic coupling, in agreement with the results of ionic model simulations. This analysis predicts that this spacing decreases with increasing steepness of CV restitution or decreasing strength of electrotonic coupling. Therefore, one important mechanism by which decreased gap junctional coupling, which is common in diseased myocardium, is proarrhythmic is through potentiation of spatially discordant alternans. Experimental studies have documented that disruption of gap junction coupling at macroscopic barriers also potentiates the formation of spatially discordant alternans,[43] which may contribute to the arrhythmogenecity of scars in ischemic heart disease.

Effects of V–Ca_i Coupling Modes on Patterns of Spatially Discordant Alternans

Recently, we have begun to explore how different modes of bidirectional coupling between voltage and Ca_i affect patterns of spatially discordant APD and Ca_i transient alternans.[44] When alternans is voltage driven by steep APD restitution slope, the spatial scales over which the APD and Ca_i transient alternans reverse phase across a nodal line are similar. This is expected because the Ca_i transient amplitude is graded with respect to APD, and the Ca_i transient in one myocyte has little influence on the Ca_i transients of its neighbors because of the slow Ca_i diffusion rate within and between cells. However, if alternans is Ca_i driven, the situation is different. Simulations[44] show that as a result of the slow diffusion of Ca_i, Ca_i alternans can reverse phase over a very short distance (less than the length of a single myocyte). In contrast, the APD of a myocyte cannot reverse phase over such a short distance because it is strongly influenced by electrotonic currents from neighboring cells (effectively limiting phase reversal to a 1- to 2-mm spatial scale corresponding to the electrical space constant of tissue). In theory, then, Ca_i-driven alternans might be distinguished from voltage-driven alternans based on whether the spatial scale over which APD reverses phase matches the spatial scale over which the Ca_i transient reverses phase. During VF in porcine ventricle, optical recordings of Ca_i between sites <2 mm apart were found to have little relationship to each other or to membrane voltage.[45] Simulations also predict that nodal lines formed during alternans should exhibit different behaviors, such as drift, depending on whether the underlying mechanism of their formation is voltage or Ca_i driven.[44] These issues are just beginning to be explored experimentally.

One of the most intriguing aspects of Ca_i alternans is the prediction that it can occur at the subcellular scale, with Ca_i in one region of a myocyte alternating out-of-phase with nearby regions,[46] as has been observed experimentally in both isolated myocytes[22,24] and intact ventricular tissue.[47] Analogous to spatially discordant APD alternans arising from a ectopic beat (Figure 7B), subcellular Ca_i alternans could arise from spatially homogeneous Ca_i alternans if a localized spontaneous SR Ca release event reset the phase of Ca_i alternans release in that region of the myocyte. However, theoretical analysis also predicts subcellular alternans can arise spontaneously in the case positive V→Ca coupling linked with negative Ca→V coupling by a Turing-like mechanism.[46]

In summary, the interactions between voltage-driven and Ca_i-driven instabilities produce a richness of dynamical phenomena at both the cellular and tissue levels that are just beginning to be experimentally explored.

Summary and Conclusions

During spatially discordant alternans, the APD and Ca_i transient alternate out of phase in different regions of the heart, creating new as well as markedly enhancing any pre-existing dispersion of refractoriness. Under these conditions, ectopic beats have a high probability of inducing re-entry. At the cellular level, either membrane voltage or Ca_i cycling instabilities can drive APD and Ca_i transient alternans. Voltage-driven alternans occurs with steep APD restitution slope, and Ca_i-driven alternans is promoted by two factors: a steep dependence of SR Ca release on SR Ca load (as occurs with SR Ca_i overload) and reduced ability of the SR to sequester Ca (attributable to either reduced SERCA pump activity or increased SR leakiness). The latter two factors are likely to account for pulsus alternans and T wave alternans in heart failure and acute myocardial ischemia. The increased predisposition to spatially discordant APD alternans also contributes to the increased arrhythmia risk in these settings. At the tissue level, voltage-driven or Ca_i-driven alternans combines with CV restitution or other factors to cause alternans to become spatially discordant, which markedly increases the probability that an ectopic beat will induce re-entry and can also induce re-entry directly.

Clinical Implications

Returning to the question posed in the Introduction, "What makes that one-in-a-million ectopic beat that induces VT/VT and SCD so special?" the evidence presented in this review suggests an answer: it is not the ectopic beat that is special; rather, it is the dynamic state of the substrate that the ectopic beat encounters that is special. Spatially discordant alternans is one of the major factors creating this special substrate by dynamically exacerbating pre-existing tissue heterogeneity, allowing the one-in-a-million ventricular ectopic beat(s) or rapid heart rates to initiate VT/VF and SCD. From this vantage point, it is not surprising that the "PVC Hypothesis" (ie, that suppression of premature ventricular contractions should prevent initiation of VT/VF and hence reduce SCD) failed as an effective antiarrhythmic strategy in large-scale clinical trials[48] because the more relevant issue is how these drugs affect the substrate rather than how they affect ventricular

ectopy. The Na channel blockers studied in the Cardiac Arrhythmia Suppression Trial (CAST),[48] for example, exaggerate CV restitution,[40,49] which directly promotes spatially discordant alternans.[41] K channel blockers such as D-sotolol studied in the Survival With Oral D-Sotalol (SWORD) trial[50] steepen APD restitution, also enhancing the onset of alternans.

Currently available clinical methodology to detect T wave alternans has already proved useful for assessing SCD risk and need for ICD implantation in patients with reduced ejection fraction.[8] In the future, improved methods to detect spatially discordant alternans in the diseased heart could provide an early warning system for identifying periods of high vulnerability to lethal arrhythmias, potentially allowing therapeutic interventions to be deployed. Current methods to detect repolarization alternans are limited in this regard because clinical algorithms for detecting T wave alternans do not indicate whether APD alternans is spatially concordant or discordant. Given the importance of CV restitution to spatially discordant alternans, for example, a refined algorithm to detect simultaneous QRS alternans (reflecting engagement of CV restitution) and T wave alternans (reflecting APD alternans) might improve predictive accuracy.[10,11] As the marriage of computational approaches with experiments provide further insights into this dynamic substrate, novel therapeutic approaches are likely to be forthcoming.

Acknowledgments

This work was supported by National Institutes of Health/National Heart, Lung, and Blood Institute grants P01 HL078931 and P50 HL53219, the Laubisch, Kawata, and Price endowments. We also thank Scott T. Lamp and Tan K. Duong for technical assistance.

References

1. Moss AJ, Zareba W, Hall WJ, Klein H, Wilber DJ, Cannom DS, Daubert JP, Higgins SL, Brown MW, Andrews ML; Multicenter Automatic Defibrillator Implantation Trial II Investigators. Prophylactic implantation of a defibrillator in patients with myocardial infarction and reduced ejection fraction. *N Engl J Med.* 2002;346:877–883.
2. Stevenson WG, Stevenson LW, Weiss J, Tillisch JH. Inducible ventricular arrhythmias and sudden death during vasodilator therapy of severe heart failure. *Am Heart J*. 1988;116:1447–1454.
3. Traube L. Ein fall von pulsus bigeminus nebst bemerkungen tiber die lebershwellungen bei klappenfehlern und uber acute leberatrophic. *Ber Klin Wschr.* 1872;9:185.
4. Lewis T. Notes upon alternation of the heart. *Quart J Med*. 1910;4: 141–144.
5. Walker ML, Rosenbaum DS. Repolarization alternans: implications for the mechanism and prevention of sudden cardiac death. *Cardiovasc Res*. 2003;57:599–614.
6. Rosenbaum DS, Jackson LE, Smith JM, Garan H, Ruskin JN, Cohen RJ. Electrical alternans and vulnerability to ventricular arrhythmias. *N Engl J Med*. 1994;330:235–241.
7. Gehi AK, Stein RH, Metz LD, Gomes JA. Microvolt T-wave alternans for the risk stratification of ventricular tachyarrhythmic events: a meta-analysis. *J Am Coll Cardiol*. 2005;46:75–82.
8. Bloomfield DM, Bigger JT, Steinman RC, Namerow PB, Parides MK, Curtis AB, Kaufman ES, Davidenko JM, Shinn TS, Fontaine JM. Microvolt T-wave alternans and the risk of death or sustained ventricular arrhythmias in patients with left ventricular dysfunction. *J Am Coll Cardiol*. 2006;47:456–463.
9. Watanabe MA, Fenton FH, Evans SJ, Hastings HM, Karma A. Mechanisms for discordant alternans. *J Cardiovasc Electrophysiol*. 2001;12: 196–206.
10. Pastore JM, Girouard SD, Laurita KR, Akar FG, Rosenbaum DS. Mechanism linking T-wave alternans to the genesis of cardiac fibrillation. *Circulation*. 1999;99:1385–1394.
11. Qu Z, Garfinkel A, Chen PS, Weiss JN. Mechanisms of discordant alternans and induction of reentry in simulated cardiac tissue. *Circulation*. 2000;102:1664–1670.
12. Henry H, Rappel WJ. Dynamics of conduction blocks in a model of paced cardiac tissue. *Phys Rev E Stat.* 2005;71:051911.
13. Wan X, Laurita KR, Pruvot EJ, Rosenbaum DS. Molecular correlates of repolarization alternans in cardiac myocytes. *J Molec Cell Cardiol*. 2005; 39:419–428.
14. Cao JM, Qu Z, Kim YH, Wu TJ, Garfinkel A, Weiss JN, Karagueuzian HS, Chen PS. Spatiotemporal heterogeneity in the induction of ventricular fibrillation by rapid pacing: importance of cardiac restitution properties. *Circ Res*. 1999;84:1318–1331.
15. Nolasco JB, Dahlen RW. A graphic method for the study of alternation in cardiac action potentials. *J Appl Physiol*. 1968;25:191–196.
16. Franz MR. The electrical restitution curve revisited: steep or flat slope—which is better? *J Cardiovasc Electrophysiol*. 2003;14:S140–7.
17. Watanabe M, Otani NF, Gilmour RF. Biphasic restitution of action potential duration and complex dynamics in ventricular myocardium. *Circ Res*. 1995;76:915–921.
18. Tolkacheva EG, Schaeffer DG, Gauthier DJ, Krassowska W. Condition for alternans and stability of the 1:1 response pattern in a "memory" model of paced cardiac dynamics. *Phys Rev E.* 2003;67:031904.
19. Pruvot EJ, Katra RP, Rosenbaum DS, Laurita KR. Role of calcium cycling versus restitution in the mechanism of repolarization alternans. *Circ Res*. 2004;94:1083–1090.
20. Goldhaber JI, Xie LH, Duong T, Motter C, Khuu K, Weiss JN. Action potential duration restitution and alternans in rabbit ventricular myocytes: the key role of intracellular calcium cycling. *Circ Res*. 2005;96:459–466.
21. Chudin E, Goldhaber J, Garfinkel A, Weiss J, Kogan B. Intracellular Ca dynamics and the stability of ventricular tachycardia. *Biophys J*. 1999; 77:2930–2941.
22. Hüser J, Wang YG, Sheehan KA, Cifuentes F, Lipsius SL, Blatter LA. Functional coupling between glycolysis and excitation-contraction coupling underlies alternans in cat heart cells. *J Physiol*. 2000;524: 795–806.
23. Diaz ME, Eisner DA, O'Neill SC. Depressed ryanodine receptor activity increases variability and duration of the systolic Ca transient in rat ventricular myocytes. *Circ Res*. 2002;91:585–593.
24. Diaz ME, O'Neill SC, Eisner DA. Sarcoplasmic reticulum calcium content fluctuation is the key to cardiac alternans. *Circ Res*. 2004;94: 650–656.
25. Pruvot E, Katra RP, Rosenbaum DS, Laurita KR. Calcium cycling as mechanism of repolarization alternans onset in the intact heart. *Circulation*. 2002;106:191–192.
26. Taggart P, Sutton PM, Boyett MR, Lab M, Swanton H. Human ventricular action potential duration during short and long cycles. Rapid modulation by ischemia. *Circulation*. 1996;94:2526–2534.
27. Qian YW, Clusin WT, Lin SF, Han J, Sung RJ. Spatial heterogeneity of calcium transient alternans during the early phase of myocardial ischemia in the blood-perfused rabbit heart. *Circulation*. 2001;104:2082–2087.
28. Shiferaw Y, Watanabe M, Garfinkel A, Weiss J, Karma A. Model of intracellular calcium cycling in ventricular myocytes. *Biophys J*. 2003; 85:3666–3686.
29. Bassani JW, Yuan W, Bers DM. Fractional SR. Ca release is regulated by trigger Ca and SR Ca content in cardiac myocytes. *Am J Physiol*. 1995; 268:C1313–C1319.
30. Dumitrescu C, Narayan P, Efimov IR, Cheng Y, Radin MJ, McCune SA, Altschuld RA. Mechanical alternans and restitution in failing SHHF rat left ventricles. *Am J Physiol.* 2002;282:H1320–H1326.
31. Kameyama M, Hirayama Y, Saitoh H, Maruyama M, Atarashi H, Takano T. Possible contribution of the sarcoplasmic reticulum Ca pump function to electrical and mechanical alternans. *J Electrocardiol*. 2003;36: 125–135.
32. Wehrens XH, Lehnart SE, Marks AR. Intracellular calcium release and cardiac disease. *Annu Rev Physiol*. 2005;67:69–98.
33. Shiferaw Y, Sato D, Karma A. Coupled dynamics of voltage and calcium in paced cardiac cells. *Phys Rev E.* 2005;71:021903.
34. Gilmour RF, Otani NF, Watanabe MA. Memory and complex dynamics in cardiac Purkinje fibers. *Am J Physiol*. 1997;41:H1826–H1832.
35. Otani NF, Gilmour RF Jr. Memory models for the electrical properties of local cardiac systems. *J Theor Biol*. 1997;187:409–436.

36. Sah R, Ramirez RJ, Oudit GY, Gidrewicz D, Trivieri MG, Zobel C, Backx PH. Regulation of cardiac excitation-contraction coupling by action potential repolarization: role of the transient outward potassium current (I(to)). *J Physiol*. 2003;546:5–18.
37. Harris DM, Mills GD, Chen X, Kubo H, Berretta RM, Votaw VS, Santana LF, Houser SR. Alterations in early action potential repolarization causes localized failure of sarcoplasmic reticulum Ca release. *Circ Res*. 2005;96:543–550.
38. Joyner RW, Ramza BM, Osaka T, Tan RC. Cellular mechanisms of delayed recovery of excitability in ventricular tissue. *Am J Physiol*. 1991;260:H225–H233.
39. Pu J, Boyden PA. Alterations of Na currents in myocytes from epicardial border zone of the infarcted heart. A possible ionic mechanism for reduced excitability and postrepolarization refractoriness. *Circ Res*. 1997;81:110–119.
40. Pu J, Balser JR, Boyden PA. Lidocaine action on Na currents in ventricular myocytes from the epicardial border zone of the infarcted heart. *Circ Res*. 1998;83:431–440.
41. Qu Z, Karagueuzian HS, Garfinkel A, Weiss JN. Effects of Na channel and cell coupling abnormalities on vulnerability to reentry: a simulation study. *Am J Physiol*. 2004;286:H1310–H1321.
42. Echebarria B, Karma A. Instability and spatiotemporal dynamics of alternans in paced cardiac tissue. *Phys Rev Lett*. 2002;88:208101.
43. Pastore JM, Rosenbaum DS. Role of structural barriers in the mechanism of alternans-induced reentry. *Circ Res*. 2000;87:1157–1163.
44. Shiferaw Y, Sato D, Garfinkel A, Qu Z, Weiss JN, Karma A. Spatially discordant alternans in cardiac tissue: the role of calcium cycling. *Heart Rhythm*. 2005;2:S58 (abstract).
45. Omichi C, Lamp ST, Lin SF, Yang J, Baher A, Zhou S, Attin M, Lee MH, Karagueuzian HS, Kogan B, Qu Z, Garfinkel A, Chen PS, Weiss JN. Intracellular Ca dynamics in ventricular fibrillation. *Am J Physiol*. 2004; 286:H1836–H1844.
46. Shiferaw Y, Karma A. Turing instability mediated by voltage and calcium diffusion in paced cardiac cells. *Proc Natl Acad Sci U S A*. 2006;In press.
47. Aistrup G, Kelly JE, Sysman-Wolpin I, Kapur S, Wasserstrom JA. Ca alternans takes three distinct forms in left ventricular myocardium. *CIrculation*. 2005;112(suppl II):II–76 (abstract).
48. Moss AJ; CAST Investigators. Effect of encainide and flecainide on mortality in a random trial of arrhythmia suppression after myocardia infarction. *N Engl J Med*. 1989;321:406–412.
49. Restivo M, Yin H, Caref EB, Patel AI, Ndrepepa G, Avitable MJ, Assadi MA, Isber N, el-Sherif N. Reentrant arrhythmias in the subacute infarction period. The proarrhythmic effect of flecainide acetate on functional reentrant circuits. *Circulation*. 1995;91:1236–1246.
50. Waldo AL, Camm AJ, deRuyter H, Friedman PL, Macneil DJ, Pauls JF, Pitt B, Pratt CM, Schwartz PJ, Veltri EP. Effect of d-sotalol on mortality in patients with left ventricular dysfunction after recent and remote myocardial infarction. *Lancet*. 1996;348:7–12.